Received: 27 June 2023 | Revised: 1 September 2023 | Accepted: 12 September 2023

DOI: 10.1002/cyto.a.24796

ORIGINAL ARTICLE

MIFlowCyt

ISAC INTERNATIONAL SOCIETY FOR ADVANCEMENT OF CYTOMETRY

CYTOMETRY Journal of Quantitative Cell Science PART A

Optimization and validation of in vivo flow cytometry chimeric antigen receptor T cell detection method using CD19his indirect staining

Silvia Zaninelli[1] | Cristian Meli[2,3] | Gianmaria Borleri[2] | Michele Quaroni[4,5] | Chiara Pavoni[2] | Giuseppe Gaipa[4,5] | Andrea Biondi[4,5,6] | Martino Introna[1] | Josée Golay[1] | Alessandro Rambaldi[2,7] | Benedetta Rambaldi[2]

[1]Division of Hematology, Center of Cellular Therapy "G. Lanzani", ASST Papa Giovanni XXIII Hospital, Bergamo, Italy

[2]Hematology and Bone Marrow Transplant Unit, ASST Papa Giovanni XXIII Hospital, Bergamo, Italy

[3]Master of Science Programme in Biology Applied to Research in Biomedicine, Facoltà di Scienze e Tecnologie, Università degli Studi di Milano, Milan, Italy

[4]Laboratory of Cell and Gene Therapy Stefano Verri, Fondazione IRCCS San Gerardo dei Tintori, Monza, Italy

[5]M. Tettamanti Center, Fondazione IRCCS San Gerardo dei Tintori, Monza, Italy

[6]Department of Pediatrics, University of Milano – Bicocca, Monza, Italy

[7]Department of Oncology and Hematology, Università degli Studi di Milano, Milan, Italy

Correspondence
Benedetta Rambaldi, Hematology and Bone Marrow Transplant Unit, ASST Papa Giovanni XXIII Hospital, Piazza OMS, 1, 24121 Bergamo, Italy.
Email: brambaldi@asst-pg23.it

Funding information
Associazione Italiana per la Ricerca sul Cancro, Grant/Award Number: 22791; 5x1000 ISM, Grant/Award Number: 21147

Abstract

CD19-targeted chimeric antigen receptor T (CAR-T) cell therapy has shown unprecedented results in patients with B cell relapsed/refractory acute lymphoblastic leukemia (R/R-ALL) and B cell non-Hodgkin lymphomas where no other curative options are available. In vivo monitoring of CAR-T cell kinetics is fundamental to understand the correlation between CAR-T cells expansion and persistence with treatment response and toxicity development. The aim of this study was to define a robust, sensitive, and universal method for CAR-T cell detection using flow cytometry. We set up and compared with each other three assays for CD19 CAR-T cell detection, all based on commercially available reagents. All methods used a recombinant human CD19 protein fragment recognized by the single-chain variable fragment of the CAR construct. The two indirect staining assays (CD19his + APC-conjugated antihistidine antibody and CD19bio + APC-conjugated antibiotin antibody) showed better sensitivity and specificity compared with the direct staining with CD19-FITC, and CD19his had a better cost-effective profile. We validated CAR detection with CD19his with parallel quantitative real-time polymerase chain reaction data and we could demonstrate a strong positive correlation. We also showed that CD19his staining can be easily included in a multicolor flow cytometry panel to achieve additional information about the cell phenotype of CAR-T cell positive subpopulations. Finally, this method can be used for different anti-CD19 CAR-T cell products and for different sample sources. These data demonstrate that detection of CAR-T cells by CD19his flow cytometry staining is a reliable, robust, and broadly applicable tool for in vivo monitoring of CAR-T cells.

KEYWORDS
B-cell lymphoma, B lymphoblastic leukemia, CAR-T cell, flow cytometry

1 | INTRODUCTION

Chimeric antigen receptor T-cell (CAR-T) therapy targeting CD19 has revolutionized the treatment of hematological neoplasms, in particular for B cell relapsed/refractory acute lymphoblastic leukemia (R/R-ALL) [1, 2]. In this regard, CD19-directed CAR-T cell treatment resulted in persistence of immunological memory, trafficking to the tumor sites, and antitumor activity, which led to tumor regression and, in most of the patients, complete remission [3–5]. Since 2017, six CAR-T cell therapies have been approved by the Food and Drug Administration (FDA) and by European Medicines Agency (EMA), among which four anti-CD19 CAR-T cells [6]. All have been approved for the treatment of hematologic malignancies, including relapsed or refractory B-ALL, diffuse large B-cell non-Hodgkin lymphoma (B-NHL), follicular lymphoma (FL), mantle cell lymphoma, and multiple myeloma. Despite this rapid success, major challenges remain to be addressed such as extending the initial application to other cancer types, minimizing treatment-associated toxicities and preventing cancer relapse [7, 8].

Several studies have now defined different factors associated to treatment response, such as the importance of the T-cell intrinsic fitness, the expansion level in peripheral blood (PB), the disease status at the time of CAR-T cell infusion, and the type and number of previous treatment lines [9–15]. In the setting of chronic lymphocyte leukemia, CD19-targeted CAR-T cell products differed at transcriptional, phenotypic, and functional level in responding compared with nonresponding patients. Indeed, in patients achieving complete remission, the CAR-T cells of the infusion bag were enriched in the expression of memory-related genes, showed memory-like phenotypic characteristics, and increased ability to release interleukin 6 (IL-6) [16]. In ALL patients treated with tisagenlecleucel, the level of CAR-T cell peak expansion, measured either by quantitative polymerase chain reaction (qPCR) or by flow cytometry, was higher in responding than in nonresponding patients. Moreover, the extent of CAR-T expansion was correlated with severity of cytokine release syndrome (CRS), one of the most common side effects of immunotherapy [17]. These studies suggest that the deep characterization of the CAR-T cell product composition and the monitoring of CAR-T cell expansion can help to identify biomarkers of response and toxicity. For these reasons, European Society for Blood and Marrow Transplantation (EBMT) and Joint Accreditation Committee of ISCT and EBMT (JACIE) recommendations suggest to monitor CAR-T cell persistence at medium and long term after the infusion, however without recommending a specific method of detection [18]. The achievement of a universal and standardized assay, that could be easily applied to different laboratories and to different CAR constructs, would be desirable to amplify the knowledge on CAR-T cell treatment [19]. To detect and quantify CAR-T cell, current approaches are represented by the quantification of the CAR transgene sequence using qPCR [20] or flow cytometry [17, 21]. Different efforts were made to propose flow cytometry assays for CAR-T cell detection, not only for the anti-CD19 CAR but also for the anti-BCMA CAR [22–27].

The aims of this study were to compare three different methods to detect CAR-T cells by flow cytometry using two indirect and one direct staining approach based on the use of a CD19 recombinant protein, to validate the best performing one toward vector copy number (VCN) qPCR-based analysis and to explore new possible applications.

2 | MATERIALS AND METHODS

2.1 | Patients and samples

Samples used in this study were obtained from the first four patients treated with the highest dose of CARCIK-CD19 cells for R/R-ALL and enrolled in the Phase I/IIa clinical trial FT01CARCIK (EudraCT 2017-000900-38) [28]. Samples were collected at fixed time points as per study protocol. Additional samples were obtained from patients treated with commercial CAR-T products such as tisagenlecleucel (Kymriah®), axicabtagene ciloleucel (Yescarta®), brexucabtagene autoleucel (Tecartus®), and lisocabtagene maraleucel (Breyanzi®) as a part of routine follow up for patients treated in our center ($N = 4$). CAR-CIK and CAR-T cell monitoring collected from other human liquid fluids such as cerebrospinal fluid and pleural effusion, when clinically indicated. Additional flow cytometry tests for analytical validation were performed on leftovers. The sensitivity, specificity, and cytotoxicity assays were performed on PB samples from anonymous healthy donors (HDs; $N = 8$). Written informed consent was obtained from all participants prior to sample collection, in accordance with the Declaration of Helsinki. Protocol approval was obtained from the ethical committee of the ASST Papa Giovanni XXIII hospital.

2.2 | CARCIK-CD19 cells for in vitro assays

The sensitivity assay and the CAR^+/CAR^- populations sorting were assessed on CARCIK-CD19 cells produced according to the already described protocol [29]. Briefly, PB mononuclear cells (PBMCs) from HD buffy coat or PB, obtained after informed consent, were electroporated in the presence of two plasmids, one encoding the anti-CD19 CAR and the other for the SB11 transposase. Cells were cultured for 21 days in advanced RPMI-1640 Medium (Gibco, Thermo Fisher Scientific, Waltham, MA) supplemented with 10% heat-inactivated fetal bovine serum (FBS; Hyclone, GE Healthcare, Chicago, IL) in the presence of IL-2. At the end of the culture CAR^+ cells were purified on a magnetic column (see Supporting information S1). For the sensitivity assay, CAR^+ cells were serially diluted in untransduced CIK cells.

2.3 | Reagents for flow cytometry CAR detection

Cells were stained using the APC-conjugated AffiniPure F(ab')2 fragment goat antihuman Immunoglobulin G (IgG), Fcγ Fragment Specific, also called anti-Fc (Jackson Immunoresearch, West Grove, PA). Subsequently, three CAR detection methods were compared: (1) the human CD19 protein fused to a histidine tag (Acro biosystems, Newark, DE)

together with APC-conjugated antihistidine antibody (Miltenyi Biotec, Bergisch, Gladbach, Germany); (2) the CD19 CAR detection reagent, a biotinylated human CD19 protein, together with APC-conjugated antibiotin antibody (Miltenyi Biotec); (3) the FITC-labeled human CD19 protein (Acro biosystems). A three-color panel was designed to perform the comparison between the three CAR detection reagents. Cells were characterized with the CD45-V500 (2D1 clone) and the CD3 monoclonal antibody conjugated to FITC or APC fluorochrome (SK7 clone), the first when the CAR was stained with the APC fluorochrome and the second when it was stained with the FITC fluorochrome (all from BD biosciences, San José, CA).

CARCIK-CD19 cells were characterized with the following monoclonal antibodies in the 12-color panel: CD19-his and anti-his APC, anti-CD3-FITC (SK7 clone), anti-CD4-BV605 (RPA-T4 clone), anti-CD8-APC-H7 (SK1 clone), anti-CD45RA-PE-Cy7 (L48 clone), anti-CD62L-BV711 (SK11 clone), CD45-V500 (2D1 clone), CD279(PD-1)-PE (EH 12.1 clone), CD223(LAG-3)-APC-R700 (T47-530 clone), CD272 (BTLA)-BB700 (J168-540 clone), CD25-BV421 (M-A251 clone), and CD127-BV786 (HIL-7R-M21 clone).

2.4 | Flow cytometry staining protocol and analysis

For flow cytometry CAR detection, 200 µL of whole PB or BM were incubated with 0.25 µg of the CD19 recombinant proteinconjugated with histidine (cat. CD9-H52H2) or 2 µL of the protein conjugated with biotin (cat. 130-115-965), as suggested by manufacturer's instructions, for 15 min at room temperature. Following the incubation, the cells were washed with the buffer containing phosphate-buffered saline (PBS, Euroclone, Milan, Italy) and 1% human serum albumin (HSA, Kedrion, Barga, Italy), and then incubated with 2 µL of the antitag antibody, respectively antihistidine or antibiotin. After 15 min, cells were washed again and incubated with all the other surface markers of choice based on the panel as already reported. For the last wash, cells were incubated 5 min in 2 mL of ammonium chloride lysing solution (BD Biosciences), centrifuged and resuspended in PBS + 1%HSA buffer for the acquisition.

For the CD19 recombinant protein directly bound to FITC fluorochrome, the whole blood was first incubated with 0.25 µg of the CD19 protein (cat. CD9HF2H2), then washed and incubated with the surface markers following the same procedure as before.

For multicolor-flow cytometry panel we started form 1 mL of blood incubated with 9 mL of ammonium chloride lysing solution (BD Biosciences) for 5 min and then centrifuged before starting the staining protocol. The absolute number of $CD3^+$ cells was obtained using lyse/no-wash tube with beads, validated for clinical use (BD Trucount™ Absolute Counting Tubes, BD Biosciences).

The stain index was calculated as the difference between the mean fluorescent intensity (MFI) of the positive and negative population divided by two times the standard deviation of the negative population. The stain index allows the normalization of the fluorochrome brightness to the background signal.

The limit of detection (LOD) was calculated as the mean of the unspecific binding plus three times the standard deviation and the lower limit of quantification (LLOQ) as the lowest dilution with a coefficient of variation between replicates <30% [30].

Stained cells were acquired on a BD FACSLyric™ platform (BD Biosciences). For data analysis, including viSNE map, BD FACSuite™ software (BD Biosciences) as well as Cytobank software (Beckman Coulter, Brea, CA) were used as appropriate.

2.5 | Quantitative real-time PCR

DNA was extracted from PBMCs, untransduced CIK, CAR^+, and CAR^- cells using the Wizard Genomic DNA purification kit (Promega Corporation, Madison, WI) according to the manufacturer's instructions. Quantitative real-time PCR to detect the integrated copy number was performed as previously described [31]. Briefly, 100 ng of genomic DNA were analyzed using TaqMan Gene Expression Master Mix (Applied Biosystems, Waltham, MA) and TaqMan qPCR (RT-PCR System QuantStudio 3, Applied Biosystems) by comparing hRNaseP qPCR results with VCN qPCR.

RNA was extracted from untransduced CIK, CAR^+, and CAR^- purified cells using the RNeasy mini kit (QIAGEN, Hilden, Germany) according to the manufacturer's instructions. Quantitative real-time PCR was set up to detect the number of CAR mRNA copies, normalized on the housekeeping gene GUS. For the primer sequences see Supporting information S1.

2.6 | Cytotoxicity assay

CIK cells, CAR^+, and CAR^- purified cells were cocultured with the $CD19^+$ REH cell line at a 1:1 effector:target (E:T) ratio for 72 h. At the end of the culture, cells were stained with 7-AAD for viability, CD3 for the identification of the effector cells and CD10 for the target cells. After 15 min, CountBright™ absolute counting beads (Thermo Fisher, Waltham, MA) were added to the tube and cells were analyzed by flow cytometry. Absolute numbers of live target cells at the end of the assay were calculated by comparing the ratio of bead events to cell events. The percentage of cytotoxic activity was determined by dividing the absolute number of target cells at the end of the culture with the absolute number of target cells at the beginning of the experiment.

2.7 | Statistical analysis

Statistical analysis was performed using Microsoft Excel®, GraphPad Prism (GraphPad Software, San Diego, CA) and R software (version 4.3.0). Significance was determined by a two-tailed paired *t*-test and *p*-values were considered statistically significant below 0.05. Pearson correlation analysis was carried out between flow cytometry and real-time PCR test results.

3 | RESULTS

3.1 | Comparison of different CAR-T cell detection methods

The different detection methods compared in this work are schematically represented in Figure 1.

The CAR molecule expressed by CARCIK-CD19 cells is composed of an anti-CD19 single-chain fragment variable (scFv) followed by the hinge and CH2-CH3 domains derived from the human IgG1. In preclinical studies, the expression of the anti-CD19 CAR on CIK cells was successfully assessed using the APC-conjugated antihuman IgG antibody, specific for the Fcγ fragment [29]. While this antibody perfectly identifies CAR^+ cells resuspended in complete medium (RPMI supplemented with FBS), it failed to recognize the same cells in whole blood due to a strong inhibition of the antibody binding by human serum IgG (Figure 2A).

In order to detect CAR^+ cells in whole blood patient's samples, we compared three alternative CAR staining strategies. Two were based on recombinant CD19 protein conjugated respectively with a histidine (CD19his) or biotin (CD19bio) tag, followed by an appropriate APC-conjugated second-step antibody, whereas the third used a recombinant CD19 directly conjugated with FITC (CD19-FITC). While the CD19bio staining was assessed using a commercial kit by Miltenyi biotec, the CD19his staining protocol was developed in our laboratory, using commercial reagents. Different infusion bag products and PB samples, from patients infused with CARCIK-CD19 cells, were stained with the three methods in parallel. All methods could detect CAR^+ cells in infusion bags as well as in PB, with a good discrimination between the positive and negative cell population (Figure 2B).

We compared the stain index of each method and the best performing one was CD19bio + antibiotin-APC, with a mean stain index of 200.1, followed by the CD19his + antihistidine-APC (mean stain index 71.1) and the CD19-FITC (mean stain index 6.8; Figure 2C). Indeed, both the indirect staining methods were characterized by a better separation between the positive and negative populations. In terms of percentage of CAR^+ cells, the two indirect staining methods always identified comparable numbers of CAR^+ cells on different PB samples, while the direct CD19-FITC always underestimated the CAR^+ population (Figure 2D).

3.2 | CAR-T cell detection methods specificity and sensitivity

The specificity of the three methods was evaluated by assessing the nonspecific binding in PB samples from HDs. The CD19his and CD19bio indirect staining methods showed very low level of unspecific binding, being 0.06% and 0.07% CAR^+ cells, respectively, while the direct CD19-FITC staining method detected a mean of 0.53% of positive events, significantly higher compared with the other two methods ($p < 0.05$; Figure 3A). We were able to calculate the LOD for each studied method: 0.08% CAR^+ cells with CD19his, 0.14% with CD19bio and 0.88% with CD19-FITC.

To test the sensitivity of these methods, CARCIK-CD19 cells were expanded in vitro and purified to obtain a 100% CAR^+ population. Purified CAR^+ cells were serially diluted into untransduced CIK

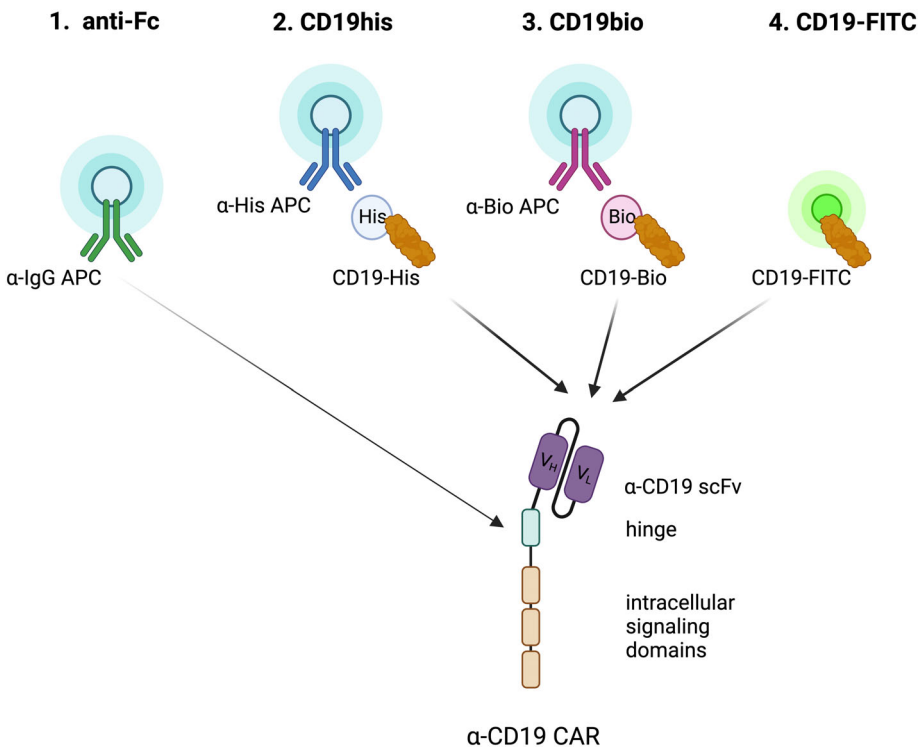

FIGURE 1 Chimeric antigen receptor (CAR) detection methods. Binding mechanisms of the different CAR detection reagents. (1) The APC-conjugated AffiniPure F(ab')2 fragment goat antihuman IgG, Fcγ fragment specific, also called anti-Fc, binds the human IgG1 derived hinge domain. (2–4) These three methods use a recombinant human CD19 protein fragment able to bind the anti-CD19 single-chain fragment variable (scFv). The CD19his (2) is fused to a histidine tag that is recognized by an APC-conjugated antihistidine antibody. The CD19bio (3) is fused to a biotin tag that is recognized by an APC-conjugated antibiotin antibody. The CD19-FITC (4) is directly conjugated to the FITC fluorochrome. [Color figure can be viewed at wileyonlinelibrary.com]

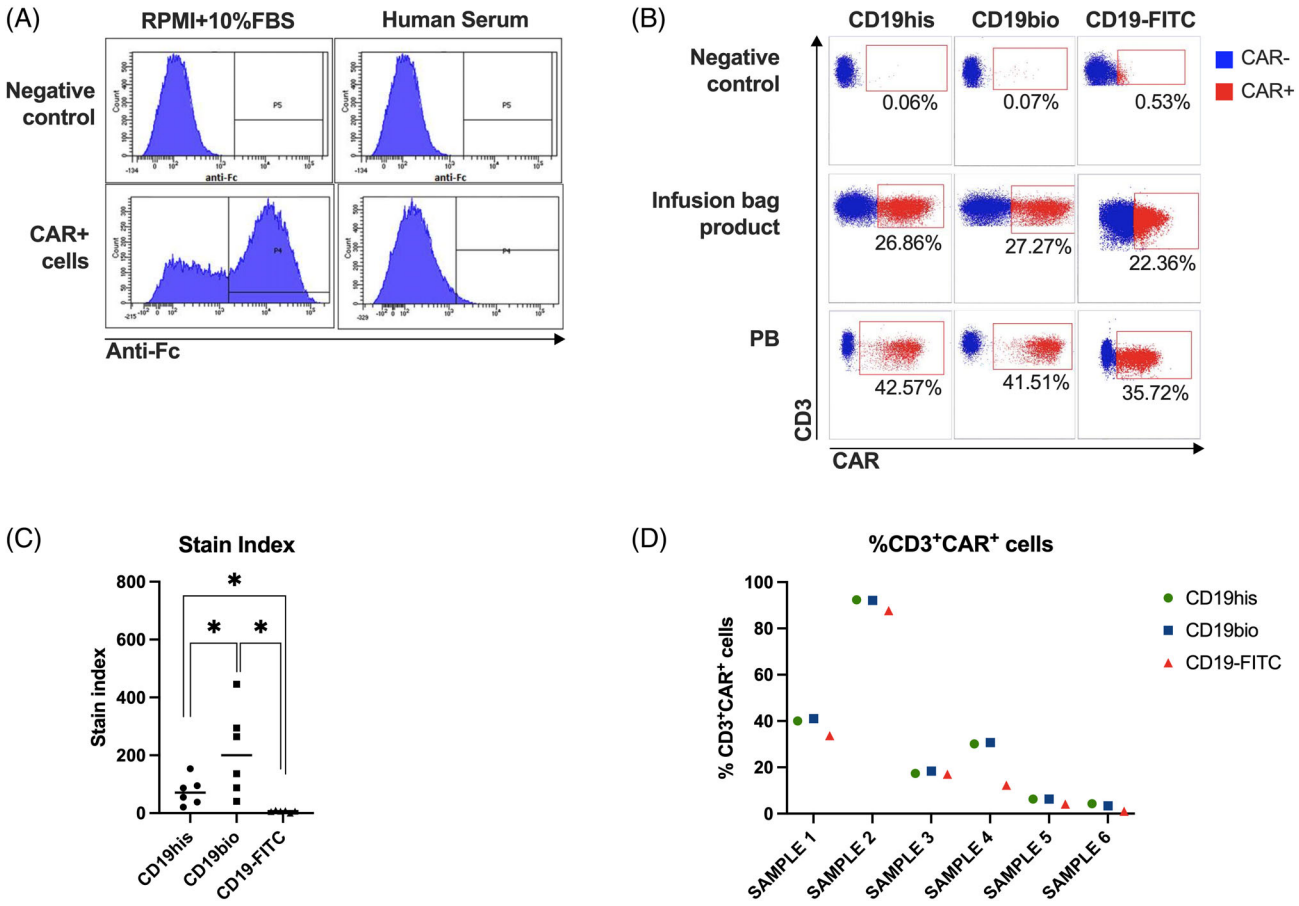

FIGURE 2 Comparison between different chimeric antigen receptor (CAR) staining methods. (A) Histograms of CARCIK-CD19 cells staining with the anti-Fc antibody in presence of complete medium (RPMI + 10% fetal bovine serum) or after 1 h incubation in human serum at 100%. Negative controls are shown in the first row and represent the unstained samples. (B) Dot plot of CARCIK-CD19 cells detection on the infusion bag product and in the peripheral blood (PB) patient sample with the three CAR detection methods. Negative controls are shown in the first row and represent the samples stained with only the secondary antibody for the indirect methods (CD19his and CD19bio), while the unstained sample for the direct method (CD19-FITC). (C) Stain index for six independent PB samples stained with the three CAR detection methods. Stain index = ((MFI CAR^+ population) − (MFI CAR^- population))/(2 × standard deviation of the CAR^- population). Bars indicate the mean of each group of samples. (D) Comparison of CD19his, CD19bio, CD19-FITC CAR staining methods in six different PB samples from patients treated with CARCIK-CD19 cells. Statistically significant differences are noted in each figure (*$p < 0.05$; two-tailed paired *t*-test). [Color figure can be viewed at wileyonlinelibrary.com]

cells, obtained from three different donors, in the presence of complete medium. Six different 10-fold dilutions were considered, from 100% to 0% CAR^+ cells. All three methods showed a similar staining pattern down to the 0.1% CAR^+ cells dilution. However, at 0.01% and 0% dilution the CD19bio displayed a lower background (Figure 3B). The dilutions were accurate as demonstrated by the R^2 for linear regression of 0.9989, 0.9990, and 0.9946 for CD19his, CD19bio, and CD19-FITC, respectively. The LLOQ of CD19his was set at 0.1%, since at this dilution the coefficient of variation between replicates was acceptable (28.23%, desired <30%) [30]. On the other hand, the coefficient of variation at 0.1% was not acceptable for CD19bio and CD19-FITC (36.42% and 40.27%, respectively) due to a higher standard deviation, requiring the definition of an higher LLOQ for these two staining methods.

3.3 | Validation of the CD19his flow cytometry staining method with VCN analysis using qPCR

Once assessed that the best performing CAR detection methods were the indirect staining methods (CD19his and CD19bio) and that there were no significant differences between them, we decided to apply the CD19his method, which had the best cost-effective profile.

In our center, CARCIK-CD19 cells were monitored on PB samples by flow cytometry and by VCN analysis at fixed time points after the infusion. We calculated the absolute number of CARCIK-$CD19^+$ cells per µL from the percentage of CARCIK-$CD19^+$ cells in the $CD3^+$ cell population, the latter being measured using absolute counting beads. Moreover, at the scheduled time points, the DNA from PBMCs was analyzed by qPCR to assess the number of anti-CD19 CAR gene

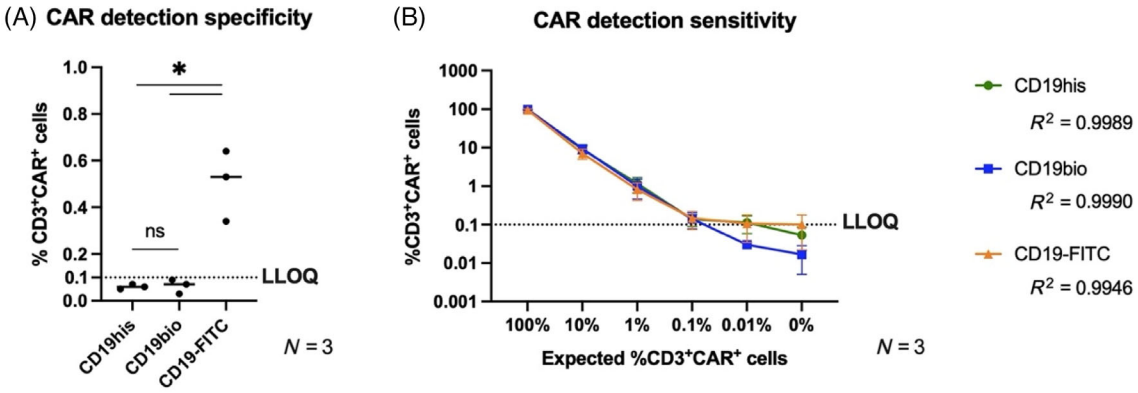

FIGURE 3 Specificity and sensitivity of the three chimeric antigen receptor (CAR) staining methods using a recombinant human CD19 protein fragment. (A) The specificity was evaluated by staining healthy donor peripheral blood mononuclear cells with the three CAR detection staining reagents to assess background staining. Data are representative of three different donors acquired in one experiment and bars indicate the mean. (B) The sensitivity was evaluated serially diluting CARCIK-CD19$^+$ cells into untransduced CIK cells at six different dilutions (from 100% to 0%). The graph shows mean values and the standard deviation of three independent experiments for each staining method (CD19his, CD19bio, CD19-FITC). The dotted line represents, in both graphs, the lower limit of quantification (LLOQ) for CD19his, identified at 0.1% CAR$^+$ cells. LLOQ was calculated as the last dilution above the limit of detection (LOD) in which the coefficient of variation between each measurement was less than 30%. The LOD was identified as the mean of the background staining plus three times the standard deviation, the LOD for CD19his was 0.08%. Statistically significant differences are noted in each figure (*$p < 0.05$; two-tailed paired *t*-test and simple linear regression). [Color figure can be viewed at wileyonlinelibrary.com]

copies per µg of DNA (VCN). To validate our flow cytometry staining method toward qPCR based VCN method, we compared the results obtained in 56 samples contemporary analyzed with both platforms. We observed a positive correlation between the two approaches, ($R = 0.51$, $p = 0.0008$) that was maintained throughout the detection range, also at low frequencies (Figure 4A–C). These results suggest that flow cytometry represents a suitable approach for CAR detection and quantification, comparable to VCN measurement using qPCR.

3.4 | Comparison of CAR expression measured with flow cytometry and qPCR

To analyze the correlation between the CAR protein expression on the cell surface, detected by flow cytometry, and the CAR VCN measured by qPCR, CARCIK-CD19 cells were purified for CAR expression on a magnetic column and the positive and negative populations analyzed by qPCR. After the selection, we obtained a mean of 99.8% and 98.5% purity in the CAR$^-$ and CAR$^+$ samples, respectively, an example of separation is shown in Figure S1. Protocol details are shown in Supporting information S1. Untransduced CIK cells were used as negative control. The CAR gene integrated in the genomic DNA was significantly higher in CAR$^+$ compared with CAR$^-$ cells, with a mean of 985.5 and 254.2 copies/µg of DNA ($p = 0.03$), respectively (Figure 4D). Of note, CAR$^-$ population still showed some level of CAR gene integration, compared with untransduced CIK cells; however, not statistically significant. To determine the CAR gene expression, we measured the CAR mRNA by qPCR. CAR$^+$ cells had a significantly higher number of CAR mRNA copies, normalized on the reference gene GUS, compared wth the CAR$^-$ cells ($p = 0.003$). CAR$^-$ cells still had some level of CAR expression, while no expression was observed in the untransduced CIK cells (Figure 4E). To address if the functional activity of CARCIK-CD19 cells was dependent on the CAR expression on the surface of the cells, we assessed the cytotoxic activity of CAR$^+$ and CAR$^-$ purified cells cocultured with a CD19$^+$ cell line. At the end of the coculture, the CAR$^+$ cells reported a high cytotoxic activity, while the CAR$^-$ cells did not show any killing activity ($p = 0.003$, Figure 4F). Finally, to test the ability of the target antigen to restimulate CAR protein expression on the cell surface in the CAR$^-$ population we measured, by flow cytometry, the CAR expression after the coculture with CD19$^+$ cells, and we observed that CAR$^-$ cells remained negative for CAR expression (Figure S2).

3.5 | CARCIK-CD19 cells monitoring: 12-color panel

Our flow cytometry-based CAR detection panel, initially assessed as a 3-color panel, was implemented as a 12-color panel, allowing a deeper characterization of the circulating CAR$^+$ cells in term of CD4/CD8, maturation subset (naïve/memory, using CD45RA and CD62L) and activation/exhaustion markers (CD25, BTLA, PD1, and LAG3). To interpret high-dimensional single-cell data produced by this multicolor flow cytometry 12-color panel, we used a tool based on the viSNE algorithm [32], which allows visualization of high-dimensional cytometry data on a two-dimensional map at single-cell resolution and preserve the nonlinearity [33], In the viSNE map, cell position reflects their proximity in high-dimensional space based on the similarity of marker expression. Figure 5 shows the evolution of CD3$^+$ CAR$^+$ and CD3$^+$ CAR$^-$ cells in a patient treated with CARCIK-CD19 cells at

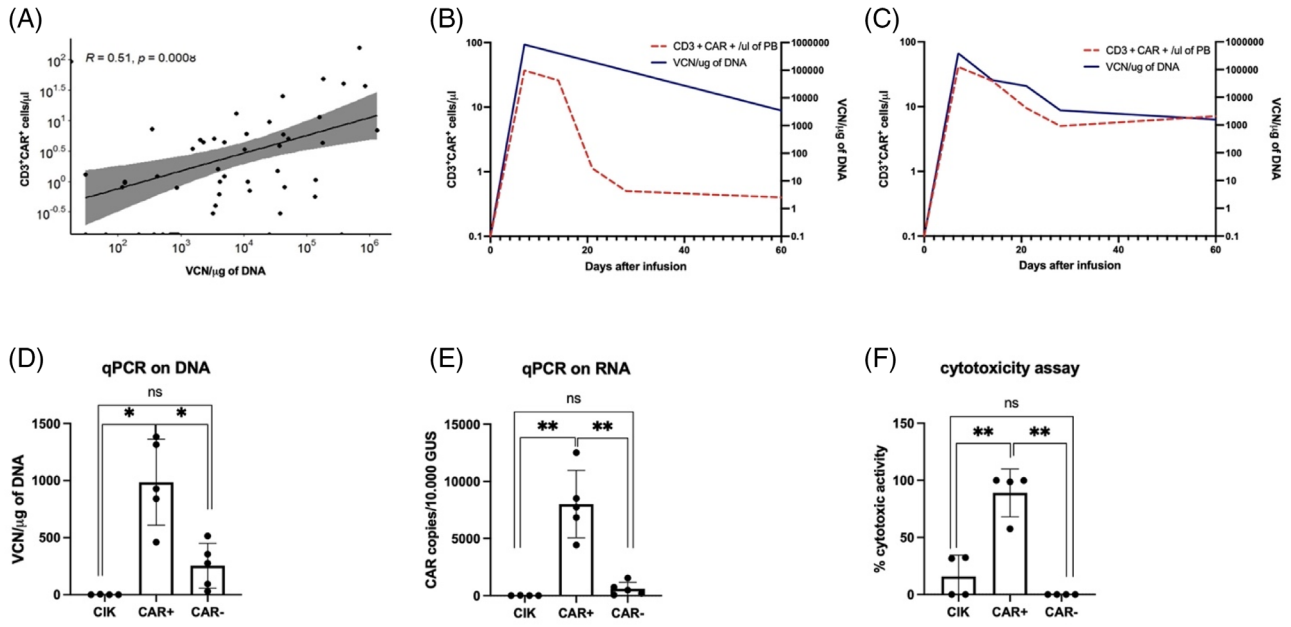

FIGURE 4 Comparison between chimeric antigen receptor (CAR) expression measured with CD19his flow cytometry and real-time polymerase chain reaction (PCR) data. (A) CAR detection was concurrently assessed in 56 postinfusion peripheral blood samples from 4 patients treated with CARCIK-CD19 cells by flow cytometry using the CD19his method ($CD3^+CAR^+$ cell/µL) and qPCR (VCN/µg of DNA). The results show clear inter-method concordance by Pearson correlation test ($R = 0.51$, $p = 0.0008$). Data are displayed in a logarithmic scale to better represent values <1 cell/µL. (B,C) Monitoring of CARCIK-CD19 expansion, using CD19his flow cytometry staining and qPCR, in two representative patients. (D–F) CARCIK-CD19 cells were expanded in vitro and purified on a magnetic column for CAR expression. Data are representative of five independent experiments. Untransduced CIK cells, CAR^+ and CAR^- purified cells were then analyzed by qPCR and for their cytotoxic activity. In each histograms columns represent the mean and bars the standard deviation. (D) CAR gene integration measured with quantitative PCR and expressed as vector copy number/µg of DNA. (E) CAR mRNA expression measured with qPCR and expressed as CAR mRNA copies normalized on the reference gene GUS. (F) Cytotoxic activity against a $CD19^+$ REH cell line at a 1:1 effector to target ratio, after 72 h coculture. Statistically significant differences are noted in each figure (*$p < 0.05$; **$p < 0.01$; two-tailed paired *t*-test). [Color figure can be viewed at wileyonlinelibrary.com]

different time points after infusion, using viSNE map. Interestingly, in this representative patient, we were able to observe a re-expansion at month three, concurrently with the disease relapse (see increasing of $CD8^+$ CAR^+ cells, green dots, in the first column at Months 3 and 5). In this example, it is possible not only to appreciate the expansion of the CAR^+ population but also their differentiation over time and their expression of activation/exhaustion markers. In conclusion, our flow cytometry CAR detection method can be easily incorporated in a multicolor flow cytometry panel and used for single-cell data analysis.

3.6 | Broad applicability of the CAR detection method

Using the CD19 recombinant protein to bind the anti-CD19 CAR expressed on the T-cell surface makes this CAR detection method related not to the exact CAR structure but on its antigen specificity. For this reason, it is possible to define this detection method "universal" since, in theory, can bind any anti-CD19 CAR and can be easily translated for different targets, by changing the protein used, for example with BCMA. To test its broad applicability, CD19his staining was used to monitor circulating CAR^+ cells in patients infused with different commercial anti-CD19 products, such as tisagenlecleucel (Kymriah®), axicabtagene ciloleucel (Yescarta®),brexucabtagene autoleucel (Tecartus®), and lisocabtagene maraleucel (Breyanzi®; Figure 6A). Of note, all these CAR structures are made from the same clone (FMC63) as well as our CARCIK-CD19 cells. The CD19his CAR detection method identified in both sets of patients circulating CAR-T cells with a good discrimination between the positive and negative population. The studied structures are made from the same clone but display some differences, such as the type of linker and the distance from the target. These data suggest that the CAR detection is independent from the specific CAR structure.

Moreover, the CD19his CAR detection method was successfully applied on samples collected from different human liquid fluids other than PB samples such as BM, cerebrospinal fluid, and pleural effusion (Figure 6B).

4 | DISCUSSION

The objective of this study was to optimize a flow cytometry-based method for monitoring circulating CAR-T cells in patients. To do so, we compared three different staining methods, using a recombinant

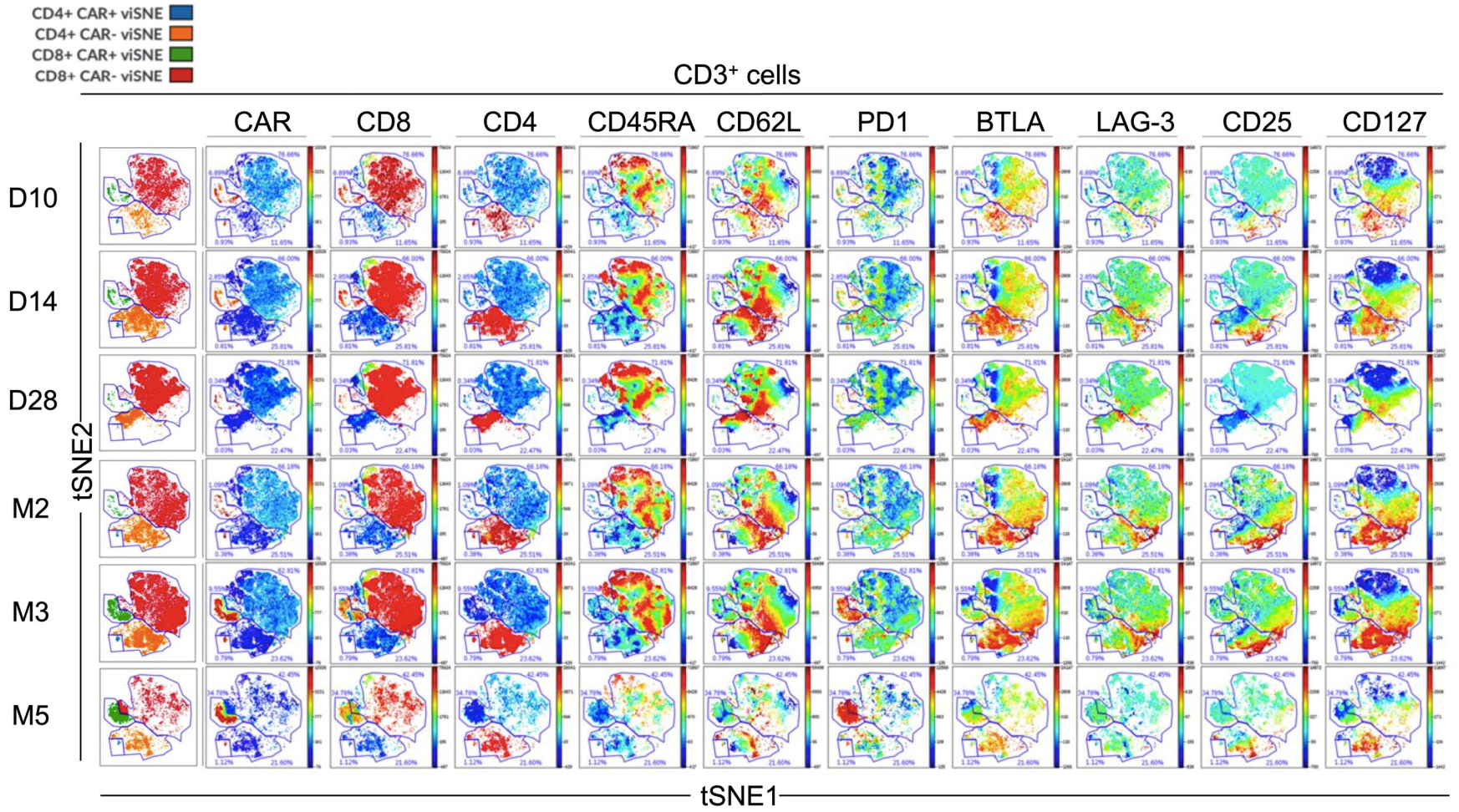

FIGURE 5 Inclusion of CD19his chimeric antigen receptor (CAR) staining method in a 12 colors flow cytometry panel. Representation of CD3 cells staining in a single patient treated with CARCIK-CD19 cells at different time point after infusion, using viSNE map visualization tool. To interpret high-dimensional single-cell data that were produced by multicolor flow cytometry panel, we used a tool based on the viSNE algorithm [32], which allows visualization of high-dimensional cytometry data on a two-dimensional map at single-cell resolution and preserve the nonlinearity [33]. In the viSNE map, cell position reflects their proximity in high-dimensional space based on the similarity of marker expression. The first column shows the distribution of the four major T-cell populations: $CD4^+$ CAR^+ cells (blue), $CD4^+$ CAR^- cells (orange), $CD8^+$ CAR^+ cells (green), and $CD8^+$ CAR^- cells (red). All the other columns show the expression level of each marker included in the panel, excluding CD45 and CD3 used for the identification of the T cells. D, day; M, month after CARCIK infusion. [Color figure can be viewed at wileyonlinelibrary.com]

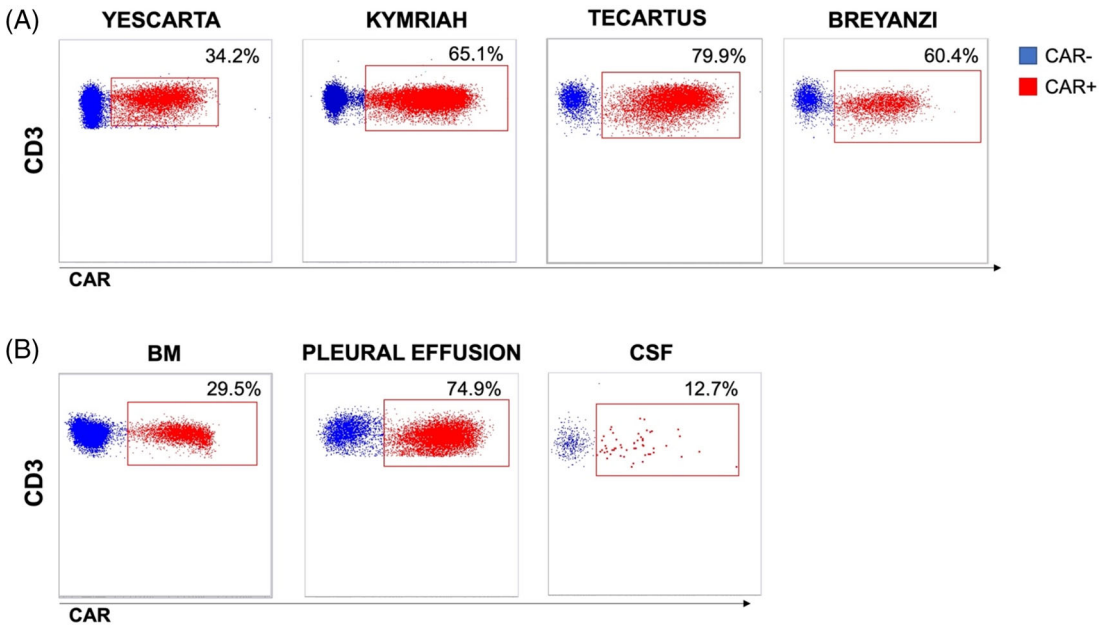

FIGURE 6 Application of the CD19his staining method on different commercial chimeric antigen receptor (CAR)-T products and within different sample sources. (A) Representative dot plots of three peripheral blood (PB) samples from patients previously infused with tisagenlecleucel (Kymriah®), axicabtagene ciloleucel (Yescarta®),brexucabtagene autoleucel (Tecartus®) and lisocabtagene maraleucel (Breyanzi®). (B) Representative dot plots of CAR detection on different sample sources: bone marrow (BM), pleural effusion and cerebrospinal fluid (CSF) in patients infused with CARCIK-CD19 cells. [Color figure can be viewed at wileyonlinelibrary.com]

human CD19 protein fragment recognized by the anti-CD19 recognition domain of the CAR construct. All three methods were able to identify the CAR-T cells in the product bags and in the PB samples of patients infused with CARCIK-CD19 cells. The two indirect staining methods using CD19his and CD19bio gave similar results and demonstrated to have higher specificity and sensitivity compared with CD19-FITC direct staining. We were able to set up the LOD at 0.08% and the LLOQ at 0.1% with CD19his, significantly lower than using the direct staining method. Moreover, CD19his is more cost-effective compared with CD19bio. For these reasons, in our center, we decided to monitor CAR-T and CARCIK-CD19 patients using CD19his as staining method.

Our flow cytometry CD19his CAR detection method was validated with parallel qPCR data. The comparison demonstrated that CD19his flow cytometry CAR detection represents a reliable and robust method to monitor CAR-T cells in patients. Indeed, also at low level of CAR positive cells per microliter, we were able to observe a correlation with the VCN data. Furthermore, in our study, we showed the correlation between VCN and absolute CAR-T cell count, and not percentage of positive cells. Indeed, absolute quantification of CAR-T cells using counting beads can directly reflect the concentration of CAR-T cells in circulation independent of the total amount of endogenous immune cells. Notably, we observed that the purified CAR^- cells showed low levels of CAR gene integration in the genomic DNA and CAR mRNA expression, that were higher compared with untransduced CIK cells. Indeed, the detection of VCN reflects only the CAR gene integration and not the actual CAR expression. mRNA transcription data in purified CAR^- cells suggest that CAR gene was partially expressed in these cells. However, functional study showed no killing activity for the CAR^- cells, suggesting that flow cytometry is a better tool to identify functionally active CAR^+ cells, expressing CAR proteins on the T-cell membrane. In addition, flow cytometry has other advantages, such as the ability to monitor not only CAR-T cell number in a rapid and cost-effective way but also the CAR-T cell phenotype and markers of homing and fitness [34].

However, qPCR is more sensitive than flow cytometry in detecting samples with a very low abundance of CAR-T cells. Also, different groups are now implementing VCN measurement with digital droplet PCR (ddPCR), showing a greater precision and sensitivity compared with qPCR in the detection of rare events with a small sample size [35–37]. Finally, studies are needed to address the prognostic impact of CAR-T cell persistence using qPCR or ddPCR compared with flow cytometry.

Different reports have shown the importance of flow cytometry for a comprehensive profiling of CAR-T cells at different stages, from product characterization during manufacturing to longitudinal evaluation of the infused product in patients [11, 15]. A deep understanding of the biological factors that affect the antitumor efficacy of CAR-T cell is crucial to improve the therapeutic responses, minimize toxicities, and maximize the clinical benefit. Therefore, the assessment of a robust CAR detection method is of crucial importance [38]. CAR-T cell expansion, either measured by flow cytometry or qPCR, commensurate with pretreatment tumor burden was the most significant determining factor for durable response [11] and CAR-T memory phenotype seems to be directly correlated to activity and persistence in patients [39–44]. In FL and diffuse large B-cell lymphoma, higher remission rates were

observed in patients with a higher in vivo CAR-T cell expansion peak and lower expression of exhaustion markers [45, 46].

Efforts were also made to correlate common hematology laboratory parameters, such as absolute lymphocyte count, to CAR-T cell expansion and related toxicities to simplify treatment monitoring. Peak expansion in lymphocyte count was concordant with CAR-T cell expansion and the absolute count was greater in responding patients. These information can help in the patient management, but are only an approximation with respect to specific CAR-T cell detection [47].

Additional tools can be used to have a more comprehensive understanding of the biological parameters influencing CAR-T cell therapy. In this regard, PB samples of patients with relapsed aggressive B-NHL and treated with Axicabtagene ciloleucel (axi-cel), were analyzed using single-cell mass cytometry (CyTOF). In this cohort, markers of T-cell activation, including Ki67 and inducible T-cell costimulator (ICOS), were significantly higher in CAR^+ and CAR^- T cells among responders [48]. Other groups are working on multiomics techniques to deeply characterize CAR-T cells. In particular, it was demonstrated that apheresis with higher proportion of naive and early memory T cells, especially in the $CD8^+$ compartment, was associated with longer CAR-T cell persistence and greater efficacy [49–52]. Single-cell sequencing studies demonstrated that CAR-T cell infusion products enriched for exhausted $CD8^+$ T cells, with low levels of TCR clonotypic diversity and deficient of T-helper 2 cells, were associated with worse responses [52–54]. However, although multiomics techniques offer a great amount of data and precisely characterize CAR-T cells, they are very expensive and time-consuming techniques that cannot be applied to daily practice.

Another advantage of the CD19his indirect staining is that it allows to easily change the detecting fluorochrome, simplifying the insertion of the CAR detection into different multicolor flow cytometry panels. Using our panel, we were able to track CAR-positive cells in the frame of 11 additional markers. Moreover, we were able to detect CARCIK-CD19 cells up to 12 months after infusion or after re-expansion at relapse [55]. On the other hand, a directly conjugated CD19 protein could further simplify the staining method and simplify its implementation. In our study, the CD19-FITC staining method demonstrated a high background and the worst separation between the negative and positive populations. Our results were concordant to the ones obtained by other groups, demonstrating the inferiority of direct methods for CAR detection [22, 25].

Finally, the CD19his staining demonstrated broad applicability, with the possibility to detect different anti-CD19 CAR-T cell constructs and within different sample sources. This peculiar characteristic has an important clinical relevance. As suggested by the EBMT and JACIE recommendations, it is crucial to monitor CAR-T cell expansion and persistence at medium and long term after the infusion [18]. One limit of our analysis is that the different anti-CD19 CAR constructs studied were all based on the same scFv clone (FMC63). Indeed, it is possible that other scFv clones might have different binding properties. Future studies are needed to test the possibility to detect different clones with the same approach. One of the greatest advantage to use flow cytometry for CAR detection is the rapidity of this test, which allows the clinicians to be aware of the results the same day of the sample collection. Moreover, it is crucial for the management of these patients to better understand the dynamic of the severe complications after the infusion. Indeed, this test can help to perform the differential diagnosis between tumor progression, infections, and direct CAR-T toxicity, such as CRS and neurotoxicity.

In conclusion, in this study, we demonstrated that the indirect CAR staining method using CD19his represent a reliable and robust tool to monitor CAR-T cells in different therapy settings. Importantly, CD19his staining method is cheap and quick, providing critical information for the clinicians in a daily manner. Also, it provides crucial data needed to improve the knowledge on this innovative immunotherapy approach. Finally, this technique might be easily translated for different CAR targets, such as BCMA or CD33 and CD123.

AUTHOR CONTRIBUTIONS

Benedetta Rambaldi: Conceptualization; writing—review and editing; writing—original draft; supervision; visualization; project administration. **Silvia Zaninelli:** Conceptualization; writing—original draft; methodology; validation; formal analysis; data curation; visualization; investigation. **Cristian Meli:** Methodology; validation; data curation. **Gianmaria Borleri:** Conceptualization; methodology; validation; data curation. **Michele Quaroni:** Data curation. **Chiara Pavoni:** Formal analysis. **Giuseppe Gaipa:** Funding acquisition; writing—review and editing; supervision. **Andrea Biondi:** Funding acquisition; writing—review and editing; supervision. **Martino Introna:** Funding acquisition; writing—review and editing; supervision. **Josée Golay:** Funding acquisition; writing—review and editing; supervision. **Alessandro Rambaldi:** Funding acquisition; writing—review and editing; supervision.

ACKNOWLEDGMENTS

The authors are grateful to all patients and HDs who kindly volunteered to participate in this study. The authors thank Anna Salvi for excellent assistance with flow cytometry analysis and Chiara Buracchi from Tettamanti research center for providing the human CD19 protein, together with APC-conjugated antibiotin antibody (Miltenyi Biotec) for CD19bio CAR detection. This work was supported by the Associazione Italiana per la Ricerca sul Cancro (Accelerator Award, project number 22791 and 5x1000 ISM project number 21147).

CONFLICT OF INTEREST STATEMENT

None of the authors have any financial interests or relationships relevant to the work described in this article.

ORCID

Benedetta Rambaldi https://orcid.org/0000-0002-5246-9471

REFERENCES

1. Sadelain M, Brentjens R, Riviere I. The basic principles of chimeric antigen receptor (CAR) design. Cancer Discov. 2013;3(4):388–98.
2. Ghorashian S, Pule M, Amrolia P. CD19 chimeric antigen receptor T cell therapy for haematological malignancies. Br J Haematol. 2015; 169(4):463–78.

3. Mueller KT, Waldron ER, Grupp SA, Levine JE, Laetsch TW, Pulsipher MA, et al. Clinical pharmacology of Tisagenlecleucel in B-cell acute lymphoblastic leukemia. Clin Cancer Res. 2018;24: 6175–84.
4. Maude SL, Laetsch TW, Buechner J, Rives S, Boyer M, Bittencourt H, et al. Tisagenlecleucel in children and Young adults with B-cell lymphoblastic leukemia. N Engl J Med. 2018;378(5):439–48.
5. Locke FL, Ghobadi A, Jacobson CA, Miklos DB, Lekakis LJ, Oluwole OO, et al. Long-term safety and activity of axicabtagene ciloleucel in refractory large B-cell lymphoma (ZUMA-1): a single-arm, multicentre, phase 1–2 trial. Lancet Oncol. 2019;20(1):31–42.
6. Chen L, Xie T, Wei B, Di DL. Current progress in CAR-T cell therapy for tumor treatment. Oncol Lett. 2022 Aug 25;24(4):358.
7. Brown CE, Mackall CL. CAR T cell therapy: inroads to response and resistance. Nat Rev Immunol. 2019;10:1–74.
8. Brudno JN, Kochenderfer JN. Recent advances in CAR T-cell toxicity: mechanisms, manifestations and management. Blood Rev. 2019 Mar; 34:45–55.
9. Guedan S, Luu M, Ammar D, Barbao P, Bonini C, Bousso P, et al. Time 2EVOLVE: predicting efficacy of engineered T-cells – how far is the bench from the bedside? J Immunother Cancer. 2022;10(5):e003487.
10. Fraietta JA, Nobles CL, Sammons MA, Lundh S, Carty SA, Reich TJ, et al. Disruption of TET2 promotes the therapeutic efficacy of CD19-targeted T cells. Nature. 2018;558(7709):307–12.
11. Locke FL, Rossi JM, Neelapu SS, Jacobson CA, Miklos DB, Ghobadi A, et al. Tumor burden, inflammation, and product attributes determine outcomes of axicabtagene ciloleucel in large B-cell lymphoma. Blood Adv. 2020;4(19):4898–911.
12. Maryamchik E, Gallagher KME, Preffer FI, Kadauke S, Maus MV. New directions in chimeric antigen receptor T cell [CAR-T] therapy and related flow cytometry. Cytometry B Clin Cytom. 2020;98(4): 299–327.
13. Golubovskaya V, Wu L. Different subsets of T cells, memory, effector functions, and CAR-T immunotherapy. Cancers (Basel). 2016;8(3):36.
14. Hong R, Hu Y, Huang H. Biomarkers for chimeric antigen receptor T cell therapy in acute lymphoblastic leukemia: prospects for personalized management and prognostic prediction. Front Immunol. 2021; 25(12):627764.
15. Lamble AJ, Myers RM, Taraseviciute A, John S, Yates B, Steinberg SM, et al. Preinfusion factors impacting relapse immunophenotype following CD19 CAR T cells. Blood Adv. 2023;7(4):575–85.
16. Fraietta JA, Lacey SF, Orlando EJ, Pruteanu-Malinici I, Gohil M, Lundh S, et al. Determinants of response and resistance to CD19 chimeric antigen receptor (CAR) T cell therapy of chronic lymphocytic leukemia. Nat Med. 2018;24(5):563–71.
17. Mueller KT, Maude SL, Porter DL, Frey N, Wood P, Han X, et al. Cellular kinetics of CTL019 in relapsed/refractory B-cell acute lymphoblastic leukemia and chronic lymphocytic leukemia. Blood. 2017; 130(21):2317–25.
18. Yakoub-Agha I, Chabannon C, Bader P, Basak GW, Bonig H, Ciceri F, et al. Management of adults and children undergoing chimeric antigen receptor T-cell therapy: best practice recommendations of the European Society for Blood and Marrow Transplantation (EBMT) and the Joint Accreditation Committee of ISCT and EBMT (JACIE). Haematologica. 2020;105(2):297–316.
19. Sarikonda G, Pahuja A, Kalfoglou C, Burns K, Nguyen K, Ch'en IL, et al. Monitoring CAR-T cell kinetics in clinical trials by multiparametric flow cytometry: benefits and challenges. Cytometry B Clin Cytom. 2021;100(1):72–8.
20. Maude SL, Frey N, Shaw PA, Aplenc R, Barrett DM, Bunin NJ, et al. Chimeric antigen receptor T cells for sustained remissions in leukemia. N Engl J Med. 2014;371(16):1507–17.
21. Turtle CJ, Hanafi LA, Berger C, Gooley TA, Cherian S, Hudecek M, et al. CD19 CAR–T cells of defined CD4+:CD8+ composition in adult B cell ALL patients. J Clin Invest. 2016;126(6):2123–38.
22. Demaret J, Varlet P, Trauet J, Beauvais D, Grossemy A, Hégo F, et al. Monitoring CAR T-cells using flow cytometry. Cytometry B Clin Cytom. 2021;100(2):218–24.
23. Johansson U, Gallagher K, Burgoyne V, Maus MV, Casey KS, Brini GG, et al. Detection of CAR-T19 cells in peripheral blood and cerebrospinal fluid: an assay applicable to routine diagnostic laboratories. Cytometry B Clin Cytom. 2021;100(6):622–31.
24. Peinelt A, Bremm M, Kreyenberg H, Cappel C, Banisharif-Dehkordi J, Erben S, et al. Monitoring of circulating CAR T cells: validation of a flow Cytometric assay, cellular kinetics, and phenotype analysis following Tisagenlecleucel. Front Immunol. 2022;13:830773.
25. Schanda N, Sauer T, Kunz A, Hückelhoven-Krauss A, Neuber B, Wang L, et al. Sensitivity and specificity of CD19.CAR-T cell detection by flow cytometry and PCR. Cell. 2021;10(11):3208.
26. Reichman A, Kunz A, Joedicke JJ, Höpken UE, Keib A, Neuber B, et al. Comparison of FACS and PCR for detection of BCMA-CAR-T cells. Int J Mol Sci. 2022;23(2):903.
27. Hu Y, Huang J. The chimeric antigen receptor detection toolkit. Front Immunol. 2020;11:1770.
28. Magnani CF, Gaipa G, Lussana F, Belotti D, Gritti G, Napolitano S, et al. Sleeping beauty–engineered CAR T cells achieve antileukemic activity without severe toxicities. J Clin Invest. 2020;130(11): 6021–33.
29. Magnani CF, Turazzi N, Benedicenti F, Calabria A, Tenderini E, Tettamanti S, et al. Immunotherapy of acute leukemia by chimeric antigen receptor-modified lymphocytes using an improved sleeping beauty transposon platform. Oncotarget. 2016;7(32):51581–97.
30. Wood B, Jevremovic D, Béné MC, Yan M, Jacobs P, Litwin V, et al. Validation of cell-based fluorescence assays: practice guidelines from the ICSH and ICCS – part V – assay performance criteria. Cytometry B Clin Cytom. 2013;84(5):315–23.
31. Magnani CF, Mezzanotte C, Cappuzzello C, Bardini M, Tettamanti S, Fazio G, et al. Preclinical efficacy and safety of CD19CAR cytokine-induced killer cells transfected with sleeping beauty transposon for the treatment of acute lymphoblastic leukemia. Hum Gene Ther. 2018;29(5):602–13.
32. Van Der ML, Hinton G. Visualizing Data using t-SNE. J Mach Learn Res. 2008;9(86):2579–605.
33. Amir E a D, Davis KL, Tadmor MD, Simonds EF, Levine JH, Bendall SC, et al. viSNE enables visualization of high dimensional single-cell data and reveals phenotypic heterogeneity of leukemia. Nat Biotechnol. 2013;31(6):545–52.
34. Lambert C, Ntrivalas E, Sack U, Flow Cytometry Working Group of the International Federation of Clinical Chemistry (IFCC). A new story for an old challenge: would flow cytometry beat molecular biology in monitoring chimeric antigen receptor T cell pharmacokinetics? Cytometry A. 2023;103(1):8–11.
35. Cheng J, Mao X, Chen C, Long X, Chen L, Zhou J, et al. Monitoring anti-CD19 chimeric antigen receptor T cell population by flow cytometry and its consistency with digital droplet polymerase chain reaction. Cytometry A. 2023;103(1):16–26.
36. Hindson CM, Chevillet JR, Briggs HA, Gallichotte EN, Ruf IK, Hindson BJ, et al. Absolute quantification by droplet digital PCR versus analog real-time PCR. Nat Methods. 2013;10(10):1003–5.
37. Franke GN, Maier J, Wildenberger K, Cross M, Giles FJ, Müller MC, et al. Comparison of real-time quantitative PCR and digital droplet PCR for BCR-ABL1 monitoring in patients with chronic myeloid leukemia. J Mol Diagn. 2020;22(1):81–9.
38. Sarikonda G, Mathieu M, Natalia M, Pahuja A, Xue Q, Pierog PL, et al. Best practices for the development, analytical validation and clinical implementation of flow cytometric methods for chimeric antigen receptor T cell analyses. Cytometry B Clin Cytom. 2021;100(1):79–91.
39. Blache U, Weiss R, Boldt A, Kapinsky M, Blaudszun AR, Quaiser A, et al. Advanced flow cytometry assays for immune monitoring of CAR-T cell applications. Front Immunol. 2021;3(12):658314.

40. McLellan AD, Ali Hosseini Rad SM. Chimeric antigen receptor T cell persistence and memory cell formation. Immunol Cell Biol. 2019; 97(7):664–74.
41. Good Z, Spiegel JY, Sahaf B, Malipatlolla MB, Ehlinger ZJ, Kurra S, et al. Post-infusion CAR TReg cells identify patients resistant to CD19-CAR therapy. Nat Med. 2022;28(9):1860–71.
42. Tan JY, Low MH, Chen Y, Lim FLWI. CAR T cell therapy in hematological malignancies: implications of the tumor microenvironment and biomarkers on efficacy and toxicity. Int J Mol Sci. 2022;23(13): 6931.
43. Shi N, Luo Y, Xu Y, Liang J, Ma A, Gan Y, et al. DAP10 predicted the outcome of pediatric B-cell acute lymphoblastic leukemia and was associated with the T-cell exhaustion. J Oncol. 2021;2021: 4824868.
44. Rossi J, Paczkowski P, Shen YW, Morse K, Flynn B, Kaiser A, et al. Preinfusion polyfunctional anti-CD19 chimeric antigen receptor T cells are associated with clinical outcomes in NHL. Blood. 2018; 132(8):804–14.
45. Lamure S, Van Laethem F, De Verbizier D, Lozano C, Gehlkopf E, Tudesq JJ, et al. Clinical and product features associated with outcome of DLBCL patients to CD19-targeted CAR T-cell therapy. Cancers (Basel). 2021;13(17):4279.
46. Caballero AC, Escribà-Garcia L, Alvarez-Fernández C, Briones J. CAR T-cell therapy predictive response markers in diffuse large B-cell lymphoma and therapeutic options after CART19 failure. Front Immunol. 2022;13:904497.
47. Faude S, Wei J, Muralidharan K, Xu X, Wertheim G, Paessler M, et al. Absolute lymphocyte count proliferation kinetics after CAR T-cell infusion impact response and relapse. Blood Adv. 2021;5(8): 2128–36.
48. Jacobson CA, Hunter BD, Redd R, Rodig SJ, Chen PH, Wright K, et al. Axicabtagene Ciloleucel in the non-trial setting: outcomes and correlates of response, resistance, and toxicity. J Clin Oncol. 2020;38(27): 3095–106.
49. Chen GM, Chen C, Das RK, Gao P, Chen CH, Bandyopadhyay S, et al. Integrative bulk and single-cell profiling of Premanufacture T-cell populations reveals factors mediating Long-term persistence of CAR T-cell therapy. Cancer Discov. 2021;11(9):2186–99.
50. Bai Z, Woodhouse S, Zhao Z, Arya R, Govek K, Kim D, et al. Single-cell antigen-specific landscape of CAR T infusion product identifies determinants of CD19-positive relapse in patients with ALL. Sci Adv. 2022;8(23):eabj2820.
51. Romain G, Strati P, Rezvan A, Fathi M, Bandey IN, Adolacion JRT, et al. Multidimensional single-cell analysis identifies a role for CD2-CD58 interactions in clinical antitumor T cell responses. J Clin Invest. 2022;132(17):e159402.
52. Yang J, Chen Y, Jing Y, Green MR, Han L. Advancing CAR T cell therapy through the use of multidimensional omics data. Nat Rev Clin Oncol. 2023;20(4):211–28.
53. Deng Q, Han G, Puebla-Osorio N, Ma MCJ, Strati P, Chasen B, et al. Characteristics of anti-CD19 CAR T-cell infusion products associated with efficacy and toxicity in patients with large B-cell lymphomas. Nat Med. 2020;26(12):1878–87.
54. Sheih A, Voillet V, Hanafi LA, DeBerg HA, Yajima M, Hawkins R, et al. Clonal kinetics and single-cell transcriptional profiling of CAR-T cells in patients undergoing CD19 CAR-T immunotherapy. Nat Commun. 2020;11:219.
55. Rambaldi B, Galimberti S, Rizzuto G, Magnani CF, Buracchi C, Risca G, et al. Carcik-CD19 cells expand In vivo toward a CD8+ memory phenotype and their persistence is associated with a longer duration of response. Blood. 2022;140(Supplement 1):10339–40.

SUPPORTING INFORMATION

Additional supporting information can be found online in the Supporting Information section at the end of this article.

How to cite this article: Zaninelli S, Meli C, Borleri G, Quaroni M, Pavoni C, Gaipa G, et al. Optimization and validation of in vivo flow cytometry chimeric antigen receptor T cell detection method using CD19his indirect staining. Cytometry. 2024; 105(2):112–23. https://doi.org/10.1002/cyto.a.24796